Proceedings of the Sixth International Conference on
Railway Technology: Research, Development and Maintenance
Edited by: J. Pombo
Civil-Comp Conferences, Volume 7, Paper 14.6
Civil-Comp Press, Edinburgh, United Kingdom, 2024
ISSN: 2753-3239, doi: 10.4203/ccc.7.14.6

Comparison of Heat Dissipation Characteristics Between Carbon Ceramic Brake Disc and Steel Brake Disc

S. Zheng[1], J. Zuo[1,2], J. Ding[1], G. Chen[1] and Y. Pan[1]

**[1]Institute of Rail Transit, Tongji University
Shanghai, China
[2]Shanghai Key Laboratory of Rail Infrastructure Durability and System Safety, Tongji University**

Abstract

In order to solve the problem of excessive temperature rise of brake discs under high-speed emergency braking conditions, carbon ceramic is being used as a new type of composite material in the development of new brake discs. By conducting fluid-solid-thermal coupling simulation, this article uses a front head train model containing brake discs to simulate the temperature changes of carbon ceramic brake discs during the braking process, meanwhile obtaining the temperature changes of the surrounding environment and comparing with the simulation results of steel brake discs. At an initial braking speed of 400km/h, surfaces of carbon ceramic brake disc can reach a maximum temperature of 1098.56K in about 86.3s, and the surrounding ambient temperature can reach a maximum of 750K.

Keywords: carbon ceramic brake disc, steel brake disc, fluid-solid-thermal coupling, heat convection, environmental temperature, high-speed train.

1 Introduction

When the train operates with a speed of 400km/h, the temperature of brake discs will reach a high-level during emergency braking [1,2], and existing brake disc materials are prone to failure under high temperature conditions [3]. Carbon ceramic, as a new type of composite material, has been used in military and aerospace fields due to its excellent application characteristics, such as good thermal stability, low wear, ultra long service life, and no heat exhaustion [4,5]. The use of carbon ceramic composite material in the manufacturing of brake discs can not only effectively reduce the unsprang mass, but also meet the needs of high-energy, high-speed, and lightweight development of trains [6,7].

Currently, researches on carbon ceramic brake discs mainly focus on improving preparation methods and material properties [8]. During the braking process, the highest temperature of carbon ceramic brake discs can reach nearly 1100K, which can have a significant impact on the surrounding environment [9]. Fluid-solid-thermal coupling simulation method is used in this article to analyse the temperature changes of brake discs and surrounding environment [10]. Under emergency braking conditions of brake discs, fluid-solid-thermal coupling can obtain real-time changes in convective heat transfer coefficient, as well as temperature changes of brake discs and surrounding environment. Results obtained through this method are more closely related to real applications. Researches of temperature changes in carbon ceramic brake discs during train braking are of great significance for the safety of trains.

2 Simulation Models

2.1 Brake Disc Models

The carbon ceramic disc brake disc used in simulation has a large difference in structure with the steel brake disc. Using SolidWorks for modelling, and in order to save computational costs and facilitate meshes, brake discs are reasonably simplified, ignoring subtle features that have a small impact on simulation results. This article analyses shaft-mounted steel brake disc used under high-speed trains. Three-dimensional models of carbon ceramic and steel brake disc are shown in Figure 1. Material parameters of the carbon ceramic brake disk are shown in Table 1, and material parameters of the steel brake disc are shown in Table 2.

Properties	Temperature	Value	Unit
Density	——	2300	kg/m^3
Specific heat capacity	373.15K	800	J/(kg*K)
	573.15K	1300	
	773.15K	1550	
	973.15K	1700	
	1173.15K	1600	
Thermal conductivity	373.15K	66.0	W/(m·k)
	573.15K	55.6	
	773.15K	51.8	
	973.15K	50.6	
	1173.15K	47.0	

Table 1: Material parameters of carbon ceramic brake disk.

Specific heat capacity[J/(kg·k)]	Density[kg/m3]	Thermal conductivity [W/(m· k)]
489.9	7980	30.9

Table 2: Material parameters of steel brake disk.

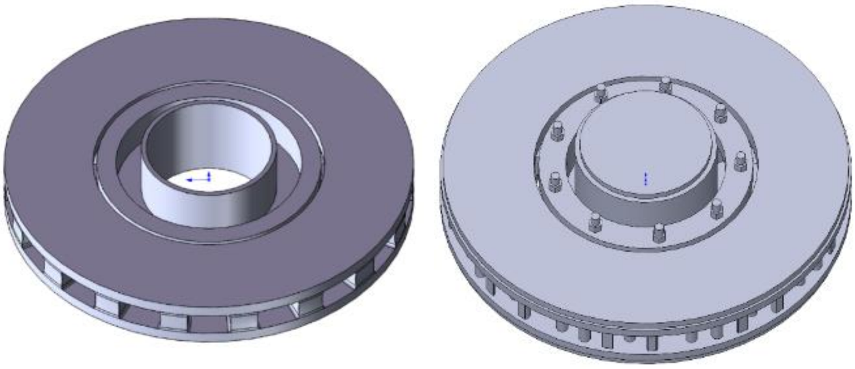

(a) (b)

Figure 1: Three-dimensional model of solid domain. (a) Carbon ceramic brake disc model. (b) Steel brake disc model.

2.2 The Front Part of Train Model

SolidWorks is used for three-dimensional modelling, on the basis of the classical model of high-speed trains to make a reasonable simplification, as far as possible to restore the real working conditions of high-speed trains during braking. The obtained model is shown in Figure 2. Set the steel brake disc and carbon ceramic brake disc models on the bogie respectively, and combine the bogie containing two types of brake discs with the front head train model to obtain train simulation models containing carbon ceramic brake discs and steel brake discs

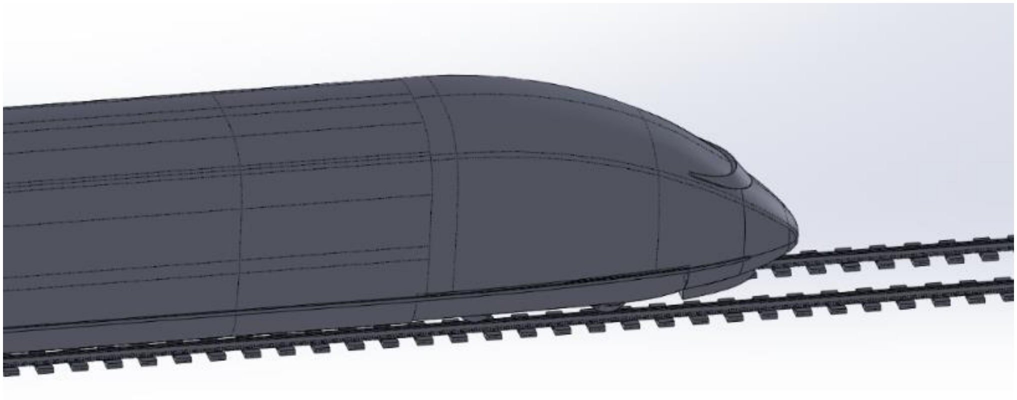

Figure 2: Simulation model of the front part of the train.

An air domain model is established around the front head of the train. The air flow field calculation domain model only retains the brake disc and a part of the axle connected to it. As shown in Figure 3, it is the fluid-solid-thermal coupling model of the steel brake disc under the front head of the high-speed train, and the carbon ceramic brake disc simulation model is the same.

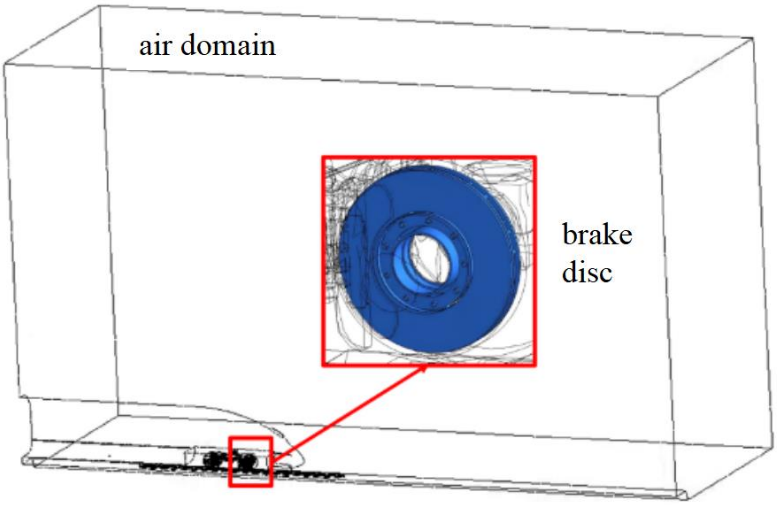

Figure 3: Air flow calculation domain model.

2.3 Simulation Mesh Division

The division of grids is crucial for simulation calculations, and the quality of grids is directly related to the convergence speed and accuracy of numerical calculations. Use ICEM-CFD to divide the model into grids, and choose unstructured grids as the grid type. In order to ensure the accuracy and reliability of the calculation results, the model has been partially encrypted in the grid. The grid density of the environment around the brake disc is higher than that of the air domain around the train.

2.4 Braking Condition and Air Parameters

The emergency braking condition is with an initial braking speed of 400km/h. The deceleration during braking is shown as Table 3. The physical parameters of air are shown in Table 4.

Velocity(km/h)	Deceleration(m/s2)
400-200	-0.98
200-0	-1.25

Table 3: Braking condition.

Specific heat capacity[J/(kg·k)]	Density[kg/m3]	Viscosity[kg/m·s]	Thermal conductivity[W/(m·k)]
1006.43	Change with temperature	1.7894e-5	0.0242

Table 4: Parameters of air.

3 Fluid-Solid-Thermal Coupling Simulation Results

3.1 Temperature Rises of the Carbon Ceramic Brake Disk and Steel Brake Disk

The emergency braking conditions with an initial speed of 400km/h are simulated. Surface temperature rise curves of the carbon ceramic brake disc and steel brake disc are shown in Figure 4. It can be seen from Figure 4 that temperature change curves all first increases and then decreases with time. This is because at the beginning, the heat input of the node is greater than the output, resulting the temperature of the node rises. At about 60s, there is a sudden change in the rate of temperature rise, which is due to the change in train deceleration, as well as the change in frictional force, resulting in a sudden change in input heat flow. When the heat input and output reach equilibrium, the temperature reaches its maximum. Then, the heat input at the node is smaller than the output, and the temperature begins to decrease. The highest temperature of carbon ceramic brake disk is 1098.56K at around 86.3s. The temperature of the steel brake disc reaches the highest at around 73s, which is 1137.62K. The specific heat capacity, thermal conductivity, and heat dissipation ability of the carbon ceramic brake disc are better than those of the steel brake disc. During the braking process, the highest temperature of the carbon ceramic brake disc will be slightly lower than that of the steel brake disc. However, when the braking is approaching the end stage, due to the thermal conduction effect of the steel brake disc, the temperature of the friction surface will decrease faster, which is lower than that of the carbon ceramic brake disc.

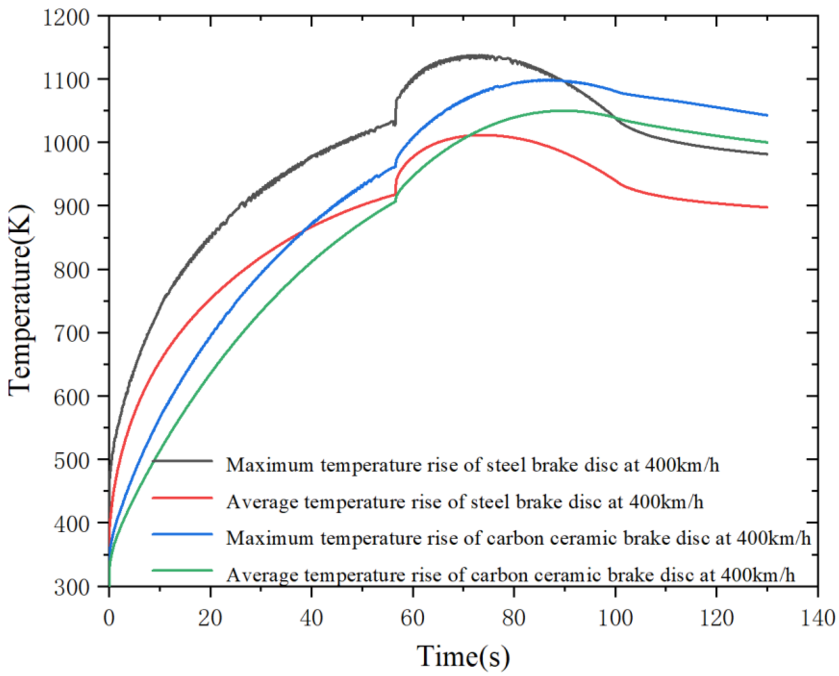

Figure 4: Temperature rise curves of carbon ceramic brake disk and steel brake disc friction surface.

3.2 Air Domain Heat Distribution Around the Carbon Ceramic Brake Disk

In order to better explore the temperature changes in the carbon ceramic brake disc and air domain inside the bogie compartment under natural convection, a working condition with an initial braking speed of 400km/h is selected. Compared to the simplified environment of brake disc thermal simulation, the simulation time is set to include the entire process from the start of braking to the end with 101s, as well as the stationary state with 29s.

During the braking process, the air inside the bogie compartment remains in a flowing state, and the flowing air continuously carries away the heat. Figure 5 shows temperature distribution cloud maps of the air domain around the carbon ceramic brake disc at different times, and the air cross-section captured in cloud maps coincide with the middle symmetry plane of the brake disc. As the braking time increases, the temperature in the air domain will also increase. However, only the air temperature around the brake disc changes significantly, and the air temperature in the area far away from the brake disc remains basically unchanged. The convection after the train braking is completed belongs to natural convection, which is different from forced convection. Air flow in natural convection is spontaneous. From the temperature distribution of the surrounding air domain at 120 seconds, it can be seen that the hot air shows an upward trend.

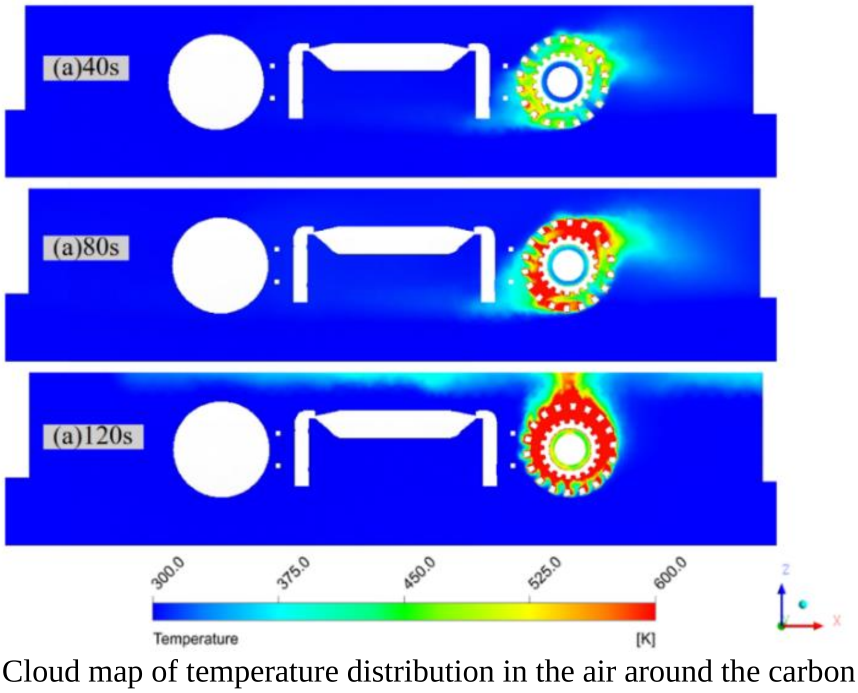

Figure 5: Cloud map of temperature distribution in the air around the carbon ceramic brake disc at different times.

3.3 Air Domain Heat Distribution Around the Steel Brake Disk

The simulation of the air domain around steel brake discs also adopts the same simulation strategy as carbon ceramic brake discs. During the braking process, the air inside the bogie compartment remains in a flowing state, and the flowing air continuously carries away the heat. Figure 6 shows temperature distribution cloud maps of the air around the steel brake disc at different times. From Figure 6, it can be seen that temperature changes around the steel brake disc are basically the same with the changes in the air domain around the carbon ceramic brake disc.

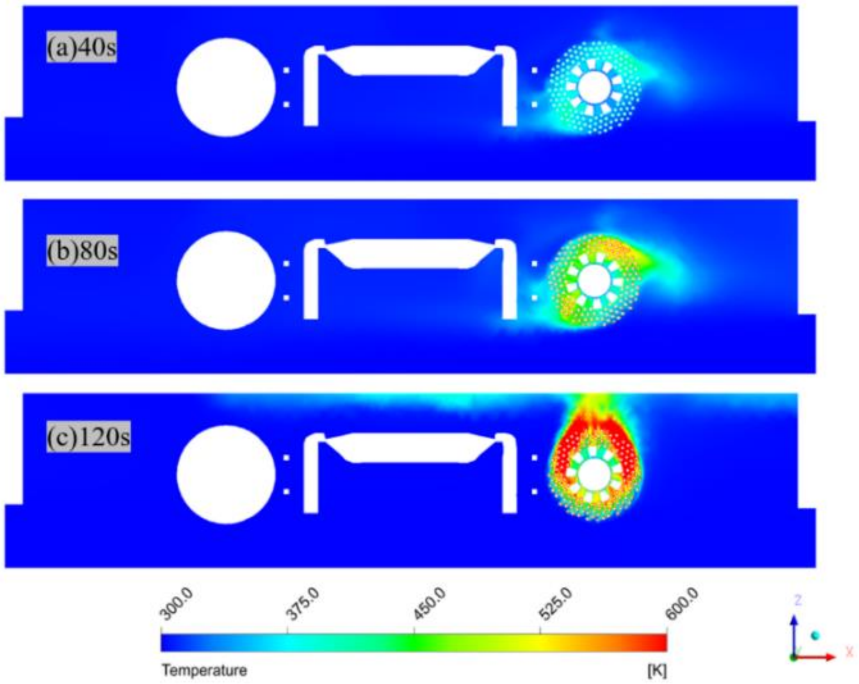

Figure 6: Cloud diagrams of temperature distribution in the air domain around steel brake discs at different times.

3.4 Comparison of Simulation Results of Heat Distribution in the Air Domain Around Carbon Ceramic Brake Discs and Steel Brake Discs

Comparing Figure 5 and Figure 6, it can be found that during the braking process, both the environment around carbon ceramic disc and steel brake disc, the thermal changes mainly occur in lower left and upper right corners of brake discs. However, due to the material characteristics and structural differences between two types of brake discs, the temperature change rate around carbon ceramic brake discs is higher than that of steel brake discs. The temperature of the air inside carbon ceramic brake discs is much higher than that of steel brake discs, and the impact on the ambient temperature directly above brake discs is more concentrated and significant after braking. When the heat flow rises to the top of the bogie area, due to higher temperature effects of carbon ceramic brake discs, the impact of carbon ceramic brake discs on the area far from the brake discs in the train's lower space is higher than that of steel brake discs, which can be clearly seen from the 120s cloud diagram.

In order to compare and analyse the impact of different brake discs on the surrounding air domain under emergency braking conditions with an initial speed of 400km/h, four nodes in the air domain located 0.1m above carbon ceramic brake discs and steel brake discs are selected, as shown in Figure 7, and output the temperature changes of these points over time.

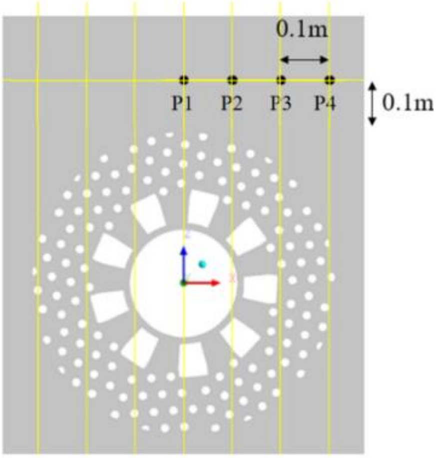

Figure 7: Schematic diagram of node location.

Temperature variation diagrams of selected air domain nodes are shown in Figure 8 and Figure 9. It can be seen that during the braking process, the node temperature gradually increases with the braking time, but the temperature change is small. After the braking is completed, the node temperature fluctuates greatly, but after a certain period of time, the temperature gradually stabilizes, reaching a stable state about 20 seconds after the train stops.

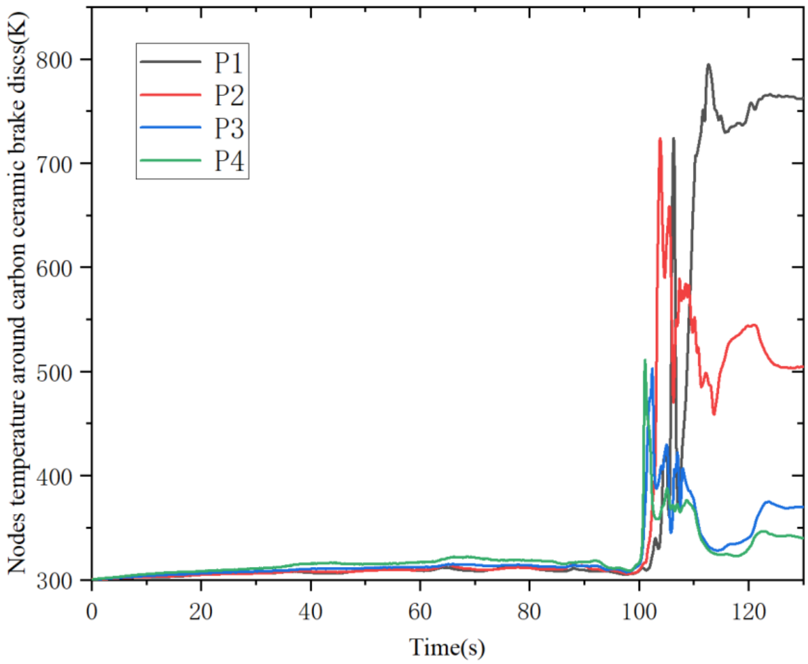

Figure 8: Temperature variation curves of nodes around carbon ceramic brake discs.

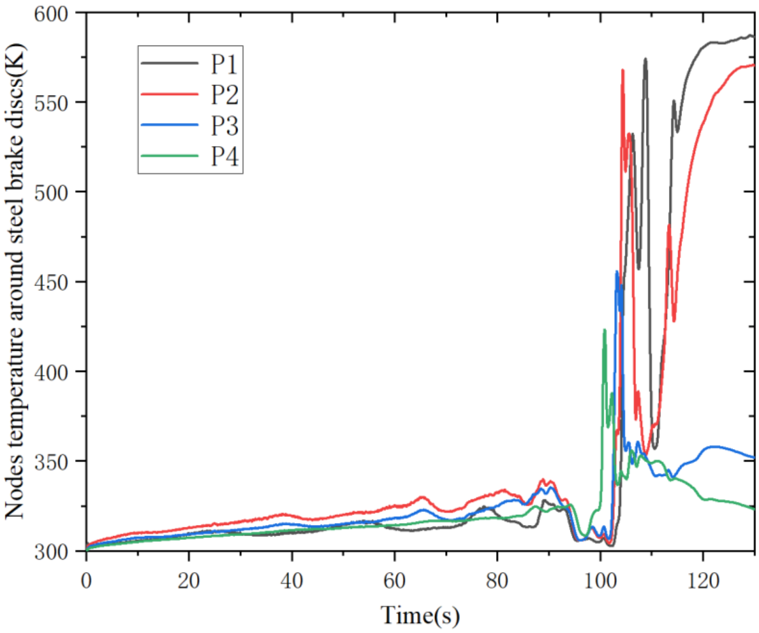

Figure 9: Temperature variation curves of nodes around steel brake discs.

Temperature at nodes p1 and p2 will be significantly higher than nodes p3 and p4, which is consistent with the simulation cloud map results of temperature distribution in the air domain. The temperature in the air domain around the carbon ceramic brake disc at P1 can reach a maximum of 800K, and maintain a stable state at 750K, which is higher than the temperature of same point around the steel brake disc. Due to small differences in temperature changes around two brake discs at nodes P3 and P4, Figure 9 shows a comparison of temperature changes between steel brake discs and carbon ceramic brake discs at nodes P1 and P2.

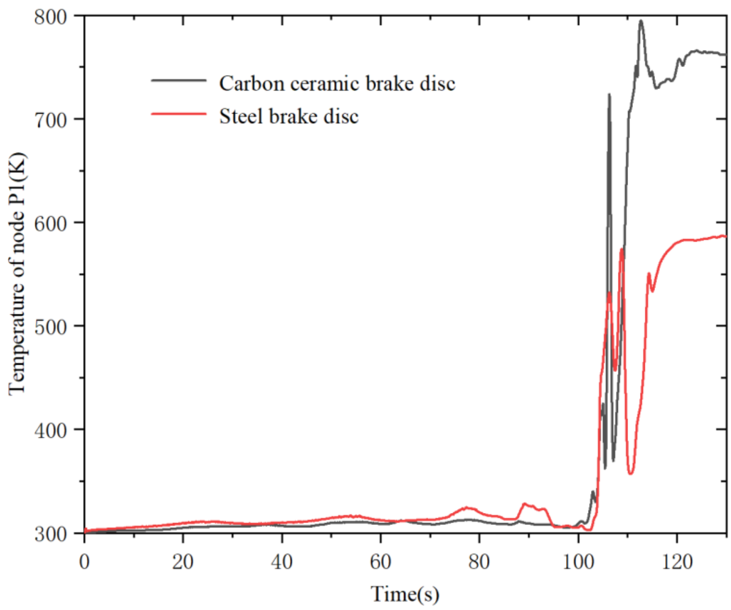

Figure 10: Temperature variation curves of P1 around carbon ceramic and steel brake discs.

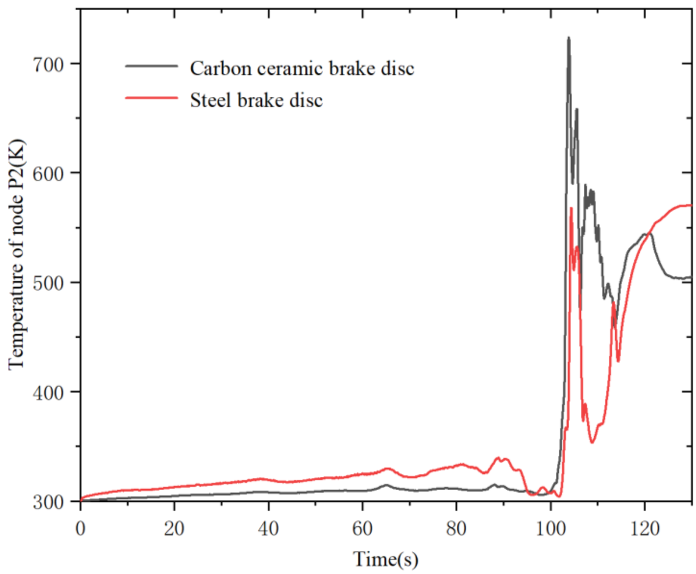

Figure 11: Temperature variation curves of P2 around carbon ceramic and steel brake discs.

It can also be found that during braking of the train, the temperature of air domain around the steel brake disc will be slightly higher than that around the carbon ceramic brake disc. It is mainly caused by the combined influence of the air flow and different brake disc structures. But when the train stops, the heat of brake discs is naturally convected outwards, temperature of the air around the carbon ceramic brake disc will be significantly higher than that of the steel brake disc. The temperature change in the surrounding environment of the carbon ceramic brake disc will be more concentrated in the middle, but the overall temperature will still be higher than that of the steel brake disc.

4 Conclusions and Contributions

By using fluid-solid-thermal coupling method, this article simulates and analyzes temperature rises of carbon ceramic brake discs and steel brake discs, and obtains the difference of temperature changes between two materials:

(1) The highest temperature of carbon ceramic brake disk is 1098.56K at around 86.3s. The temperature of the steel brake disc reaches the highest at around 73s, which is 1137.62K.

(2) During the braking process, thermal changes mainly occur in lower left and upper right corners of the environment around carbon ceramic disc and steel brake disc. The temperature of air domain around the steel brake disc will be slightly higher than that around the carbon ceramic brake disc. When the train stops, temperature of the air around the carbon ceramic brake disc will be significantly higher than that of the steel brake disc. The temperature in the air domain around the carbon ceramic brake disc can reach a maximum of 800K and maintain a stable state at 750K.

Acknowledgements

This work was supported by the National Natural Science Foundation of China (Grant No. 62273258), Science and Technology Research and Development Programme Topics of China State Railway Group Co., Ltd. (Grant No. K2023J005), and Shanghai Collaborative Innovation Research Center for Multi-network & Multi-model Rail Transit.

References

[1] A.A. Yevtushenko, "Comparative analysis of temperature fields in railway solid and ventilated brake discs", Materials, Vol.14 (2021) 7804. https://doi.org/10.3390/ma14247804.

[2] P. Ji, F. Wu, G. Zhang, X. Yin, D. Vainchtein, "A novel numerical approach for investigation of the heat transport in a full 3D brake system of high-speed trains", Numerical Heat Transfer, Part A: Applications, 75 (2019) 824–840. https://doi.org/10.1080/10407782.2019.1608767.

[3] H. Hong, M. Kim, H. Lee, I. Jo, N. Jeong, H. Moon, M. Suh, J. Lee, "A study on an analysis model for the thermo-mechanical behavior of a solid disc brake for rapid transit railway vehicles", Journal of Mechanical Science and Technology, 32 (2018) 3223–3231. https://doi.org/10.1007/s12206-018-0322-6.

[4] L. Jia, M. Wang, X. Guo, J. Zhu, A. Li, Y. Peng, "Effect of chemical vapor infiltration on the flexural properties of C/C-SiC composites prepared by the precursor infiltration pyrolysis method", Carbon, 218 (2024) 118684. https://doi.org/10.1016/j.carbon.2023.118684.

[5] Q. Chen, L. Zhu, S. Bai, Y. Ye, "Preparation and properties of highly thermal conductive C/C-SiC, Mater". Today Communication, 36 (2023) 106595. https://doi.org/10.1016/j.mtcomm.2023.106595.

[6] P. Deng, P. Li, P. Xiao, Z. Li, J. Li, P. Chen, P. Liu, F. Li, " Oxidation behaviour of C/C–SiC brake discs tested on full-scale bench rig", Ceramics International, 47 (2021) 34783–34793. https://doi.org/10.1016/j.ceramint.2021.09.017.

[7] R. Huang, J. Deng, X. Ma, Y. Mao, S. Fan, "Modifying C/C–SiC brake pads with different Fe–Si alloy phases to improve the wear resistance of full-carbon/ceramic brake pair", Ceramics International, 50 (2024) 10582–10592. https://doi.org/10.1016/j.ceramint.2023.12.370.

[8] F. Chen, Z. Li, Y. Luo, D. Li, W. Ma, C. Zhang, H. Tang, F. Li, P. Xiao, "Braking behaviors of Cu-based PM brake pads mating with C/C–SiC and 30CrMnSi steel discs under high-energy braking", Wear, 486–487 (2021) 204019. https://doi.org/10.1016/j.wear.2021.204019.

[9] P. Zhang, L. Zhu, Y. Tong, Y. Li, Y. Xing, H. Lan, Y. Sun, X. Liang, "Revealing thermal shock behaviors and damage mechanism of 3D needled C/C–SiC composites based on multi-scale analysis", Journal of Materials Research and Technology, 29 (2024) 2016–2034. https://doi.org/10.1016/j.jmrt.2024.01.260.

[10] H. Hong, M. Kim, H. Lee, N. Jeong, H. Moon, E. Lee, H. Kim, M. Suh, J. Chung, J. Lee, "The thermo-mechanical behavior of brake discs for high-speed railway vehicles", Journal of Mechanical Science and Technology, Vol.33 (2019) 1711–1721. https://doi.org/10.1007/s12206-019-0323-0.